JOURNAL OF PROPULSION AND POWER
Vol. 22, No. 3, May–June 2006

Performance Evaluation of 8-cm-diam Ion Optics Assemblies Fabricated from Carbon-Carbon Composites

Suraj P. Rawal* and Alan R. Perry†
Lockheed Martin Space Systems, Littleton, Colorado 80125
John D. Williams,‡ Paul J. Wilbur,§ and D. Mark Laufer¶
Colorado State University, Fort Collins, Colorado 80523
Wei Shih**
AllComp, Inc., City of Industry, California 91746
and
Jon Polaha†† and W. Andrew Hoskins‡‡
Aerojet-General Corporation, Redmond, Washington 98073

Performance data are presented on two sets of 8-cm-diam carbon-carbon (C-C) composite ion optics assemblies. Each C-C grid was designed and fabricated to grid feature geometries that were identical to the NSTAR ion engine, and their performance was characterized by mounting them to an 8-cm-diam plasma source. The only difference between the assemblies was that one set was dished while the other set was flat. Electron backstreaming and impingement-limited total voltage data were measured over wide beam current ranges for both the flat and dished ion optics assemblies. Electron backstreaming performance was observed to be in good agreement with NSTAR data. Impingement-limited total voltage behavior for the flat grids was observed to be similar to an 8-cm ion optics system fabricated from pyrolytic graphite. The dished grids displayed less total voltage margin because of slightly larger grid-to-grid spacing near the central regions of the assembly. Random vibration tests were successfully performed up to 29 g_{rms}, which demonstrated the structural integrity of both grid assemblies. Test data are also presented for subscale ion optics assemblies (gridlets) that were fabricated from carbon-carbon composites using the same processes used to fabricate full-size grid assemblies. The gridlets were used to characterize impingement and backstreaming limits on beamlet current over intragrid electric field conditions ranging from 2.3 to 3.4 kV/mm. The test results reported herein using carbon-carbon composites support the feasibility of directly replacing grid assemblies fabricated from molybdenum. A discussion is also presented of the anticipated lifetime enhancement afforded by carbon-based ion optics systems that show the promise of low sputter erosion rates.

Nomenclature

d	=	diameter, mm
f	=	frequency, Hz
Isp	=	specific impulse, s
J	=	current, A
j	=	current density of bombarding ions, A/m^2
ℓ	=	distance, mm
m	=	mass of an atom of a surface being sputtered by energetic ion bombardment, kg
Q	=	resonance quality factor, m/m
t	=	thickness, mm
V	=	voltage, V
Y	=	sputter yield, atoms/ion
β	=	propellant throughput enhancement factor
ρ	=	density, gm/cm^3

Subscripts

a	=	accelerator
B	=	beam
b	=	beamlet (or per aperture set quantity)
C	=	carbon
COL	=	crossover limit
cc	=	center to center
g	=	grid
Mo	=	molybdenum
min	=	minimum
n	=	natural
PL	=	perveance limit
rms	=	root mean square
s	=	screen
t	=	thickness or total

Presented as Paper 2004-3614 at the 40th Joint Propulsion Conference, Ft. Lauderdale, FL, 11–14 July 2004; received 13 September 2004; revision received 24 May 2005; accepted for publication 25 May 2005.

*Manager, MS S3085, P.O. Box 179, Research and Technology. Member AIAA.
†Senior Engineer, MS S3085, P.O. Box 179, Research and Technology. Member AIAA.
‡Assistant Professor, Mechanical Engineering, 1320 Campus Delivery. Senior Member AIAA.
§Professor, Mechanical Engineering, 1320 Campus Delivery. Senior Member AIAA.
¶Graduate Research Assistant, Mechanical Engineering, 1320 Campus Delivery. Student Member AIAA.
**President, 209 Puente Avenue. Senior Member AIAA.
††Development Engineer, Redmond Operations. Member AIAA.
‡‡Senior Staff Engineer, Redmond Operations. Member AIAA.

I. Introduction

AN 8-cm ion thruster operated at 200 mA and a net accelerating voltage of 1800 V would produce ∼13 mN of thrust at a specific impulse of ∼4000 s. If equipped with carbon-based ion optics systems, a set of three thrusters of this size could process >100 kg of propellant. A key factor that will help ensure the anticipated high propellant throughput for these small engines is a demonstration of the ability to fabricate ion optics systems from carbon-carbon (C-C) composite materials. In addition to the promise of long lifetime as a result of excellent sputter erosion resistance, carbon-based ion optics systems are lightweight and have low thermal expansion coefficients (e.g., −0.4 μm/m/K compared to 5.1 μm/m/K for molybdenum).

Regardless of the grid material, the ion current range over which a particular ion optics system can be operated is generally limited by the onset of destructive direct ion impingement at both high and low values of ion current per hole (beamlet current). These current limitations can manifest themselves during initial testing of a grid set or after many tens of thousands of hours of operation during a particular mission or acceptance/qualification test sequence. This is especially true when thrusters with wide variations in beam flatness uniformity are tested or when wide throttling ranges are involved to meet a mission requirement. To avoid damage to hardware, the ion optics characteristics of the proposed ion acceleration system must be carefully determined before a device is placed under test at a given operating condition.

When the beamlet current is low, the sheath that separates the discharge chamber plasma from the ion acceleration region is dished upstream to the point where ions are overfocused, their trajectories cross, and, at the limit, ions in the beamlet begin to impinge directly on the downstream edge of an accelerator grid aperture. A low beamlet current condition can occur at the edge of an ion optics system or over the entire optics system of a thruster that is operated at a low throttle condition, and this limiting beamlet current condition is referred to herein as the crossover limit. When the beamlet current is high, on the other hand, the sheath is dished less, and the ions can be underfocused to the point where they begin to impinge directly on the upstream side of the accelerator grid near an aperture entrance. This condition can occur in any ion optics system that is operated at excessively high beamlet currents and is referred to herein as the perveance limit. Careful attention must be paid to both of the perveance and crossover limits to prevent direct ion impingement and rapid accelerator grid erosion.[1–3]

A third and equally important operational limit on ion optics systems is the backstreaming limit, which is the voltage that must be applied to the accelerator grid to prevent beam plasma electrons from backstreaming. Ideally the accelerator grid voltage should be held negative but as close to this limit as possible. This will ensure that damage caused by the small current of charge exchange ions that sputter erode and limit the lifetime of the accelerator grid will be minimized. Unfortunately, the backstreaming limit can change as the accelerator grid wears over time or when the beam current is changed and compromises on selecting the magnitude of the accelerator voltage must be made. Many factors can affect the backstreaming voltage including aperture geometry, net voltage, and beamlet current. The plasma flowfield environment in the ion beam is also an important factor in determining the backstreaming limit.[3,4] The onset of backstreaming can also be strongly affected by the operational conditions associated with the neutralizer and conductive plasma bridge that forms between the neutralizer plasma and the beam plasma.[3] During a mission, the accelerator grid can erode to the point where the voltage limit of the accelerator power supply is no longer adequate to stop electrons from backstreaming. This condition defines the end of life for the thruster/power-supply system. To ensure that adequate margins exist at beginning of life (BOL), backstreaming limit measurements are required on proposed hardware geometry over the range of expected beamlet current.

A final consideration that can limit the operation of an ion optics assembly is the electric field applied between the grids. Long-term operation of grids fabricated from molybdenum at electric fields as high as 3.4 kV/mm appears to be feasible without excessive arcing rates or arc damage that results in lower arc threshold voltages or higher arc frequencies.[5] This level of performance over long operational times has not been demonstrated with carbon-based ion optics systems at the present time. One concern for ion optics systems fabricated from carbon fibers is the chance that cleaved fibers and/or fiber bundles might peel from a grid surface and provide a sharp point where an arc could form. To address this and other concerns, chemical-vapor-deposition processes have been developed to produce dense C-C grids with low probability of fiber failure and improved surface smoothness. C-C composites processed in this way have been operated at high voltage and high electric fields at NASA Jet Propulsion Laboratory without deleterious effects.[6]

This paper presents a preliminary look at the feasibility of designing and fabricating ion optics systems comprised of C-C composite material that show the promise of slow erosion and high arc resistance. This paper also includes a brief description of design and fabrication aspects of C-C ion engine grids, followed by a description of the experimental apparatus and procedures used to conduct tests on gridlets and full-scale C-C ion optics assemblies. Test results are presented for beamlet current limitations, backstreaming onset, and electric field standoff capability of gridlets fabricated with 109 aperture sets. The gridlet results are followed by a presentation of performance measurements made on two 8-cm-diam ion optics assemblies that were flat and dished. Both grid sets contained ~1190 aperture sets that were identical to the aperture feature geometry of NASA's Solar Electric Propulsion Technology Application Readiness (NSTAR) thruster. The grids were tested using a laboratory-model 8-cm-diam thruster. Both impingement-limited total voltage and backstreaming onset measurements were made over beam current ranges from 36 to 206 mA. Results of random vibration testing performed on flat and dished grid assemblies are also reported along with a detailed description of the test setup. Finally, a discussion of the potential life-enhancing benefits of using carbon as opposed to molybdenum grid material is presented, which takes into account recent sputter yield measurements that have been made at low xenon ion energies.[7]

II. Test Apparatus and Procedures

The following sections review the apparatus and procedures followed to perform ion optics design and fabrication, random vibration screening, gridlet testing, and full ion optics evaluation.

A. Eight-Centimeter C-C Grid Design and Fabrication

The NSTAR ion thruster system requirements were used as guidelines for the C-C grid design and development effort.[8] At a minimum, after being subjected to the launch random vibration level of 13.1 g_{rms}, the screen and accelerator grids must not remain in contact with one another. Thruster and ion-engine grid environments were used to define the grid material property requirements. Key material property requirements include 1) low erosion rate, 2) high stiffness, 3) dimensional stability, and 4) low density. Since the 1990s, several attempts have been made to demonstrate the feasibility of fabricating flat and dished carbon-based grids.[8–13] While recognizing the challenges in the areas of fabrication and machining, results of these development efforts indicated that given the appropriate aperture geometry the carbon-based grids exhibit perveance performance nearly equivalent to conventional Mo grids.

Preliminary modeling and analysis (Makowski, K., "8-cm C-C Grid Analysis," private communication, 16 Dec. 2002) was performed to quantify screen and accelerator grid displacements during random vibration testing. Results of 8-cm grid fabrication efforts and vibration analysis are shown in Fig. 1. The vibration analysis shown in Fig. 1b indicates that the maximum relative displacement caused by typical launch loads is significantly lower than the desired intragrid gap, if the dome height (dish depth) is at least 0.5 mm for grids with thin (i.e., 1-mm-thick) integral mounting flanges. When thicker (1.6-mm) mounting flanges are used, the analysis predicts that flat grids would not touch one another at random vibration test levels below 13 g_{rms}. Although the analysis shows that dishing might not be necessary, it was decided to fabricate dished grids to gain experience that might be necessary if larger diameter grid sets are to be fabricated in the future.

The dished grids used in this study had a dome height of 1.0 mm. Key steps in the processing and fabrication of the flat and dished C-C grids included 1) lay up and molding, 2) carbonization and chemical vapor deposition, 3) laser machining, and 4) application of a carbon-based seal coat. Each grid had an integral thick outer ring with 12 mounting holes to mate with an 8-cm-diam thruster.

B. Random Vibration Tests

Random vibration tests of both the flat and dished C-C grids were performed using a mounting system that simulated a thruster (Fig. 1a). Prior to vibration testing, visual and low magnification

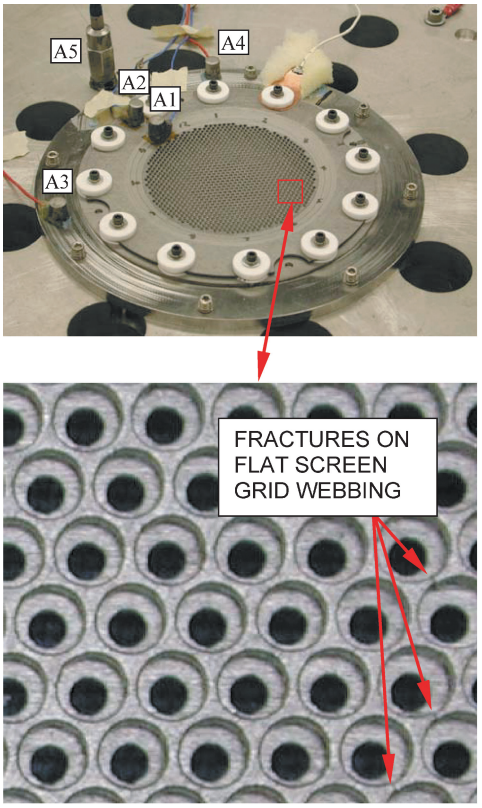

Fig. 1a Dished 8-cm C-C grid set shown attached to a vibration table along with a postvibration test photograph of the flat grid set showing web fractures that were evident prior to vibe testing. Apparent misalignment of the grids is caused by the angle of the camera relative to the subject.

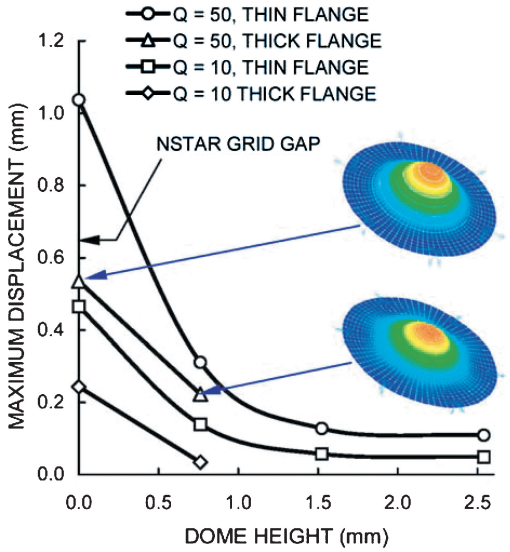

Fig. 1b Calculated maximum relative displacement between the screen and accelerator grids as a function of dome height (i.e., dish depth). The inset images show displacement of the screen grid as a function of color.

microscopic inspection of each grid was performed to evaluate its dimensional accuracy and structural integrity. The flat screen and accelerator grids looked very flat (to within ±0.0.05 mm), and laser-machined holes appeared smooth with no detectable damage in the webbing. However, microphotographs of the flat screen grid revealed the presence of several partial and/or through thickness web fractures (Fig. 1a). The fractures were arranged in a chain that followed the grid periphery for about 30 deg of the circumference. These were assumed to have occurred during either handling, machining, or transportation, and were present before vibration testing. The dished grids exhibited a dome height anomaly that caused the grid gap near the center region to be 1.2 times larger in comparison to the remaining areas. No microfractures were observed in the dished grid set either before or after the vibration tests.

Random vibration testing was based on protoflight qualification level specifications originally developed under the NSTAR program. Each grid set was mounted to the test fixture and tested to the 13 g_{rms} qualification (+3 dB above flight) level, and, subsequently, to a much higher level of 29 g_{rms} (+10 dB). Five accelerometers were placed on and nearby each of the grid sets (as shown in the photograph contained in Fig. 1a), and a continuity circuit was incorporated to detect intragrid contact during the vibration tests.

C. Subscale Ion Optics Tests

Initial ion optics testing was conducted by mounting subscale assemblies composed of two gridlet electrodes to a ring-cusp discharge chamber. The gridlets contained only a small fraction of the total number of aperture sets that are typically used in a broad area ion thruster. The use of gridlets allows one to investigate operational limits in a controlled laboratory environment. For the tests described herein, the screen and accelerator gridlets were insulated from one another using iso-mica sheets and were aligned through the use of pins and precision-placed alignment holes.

Gridlet testing involved measurement of the beam and accelerator current as the gridlet ion source discharge chamber power was varied. The discharge voltage was held at 30 V for all of the tests reported herein. The flow rate was also fixed at the start of a particular test to a value that was ~30 to 60% larger than that required to operate at the perveance limit under the prevailing beam and accelerator voltages. The gridlet tests were performed over various beam and accelerator voltages to determine the effects of throttling on crossover, perveance, and backstreaming limit data. The error in the crossover and perveance limit data was estimated to be ±0.02 and ±0.04 mA/hole, respectively. The backstreaming limit error was ±10 V. For the most part, the errors are dominated by the beamlet current step size and by the accelerator voltage step size that were chosen to record the data, but systematic errors caused by spacing the grids incorrectly (ℓ_g error ±10%) were also relatively important.

Figure 2 contains a sketch of the gridlet geometry that will be referred to herein. The dimensions of the C-C gridlets and ion optics assemblies are listed in Table 1. In addition to the nominal grid dimensions, Table 2 contains some of the beam and accelerator voltages where data were collected. The values indicated correspond to the NSTAR thruster throttle point #15 (TH15) and to the NASA Evolutionary Xenon Thruster (NEXT) high-power operating point. It is noted that the current configuration of the NEXT thruster uses an ion optics system that is identical in aperture feature geometry to the NSTAR engine except for the accelerator grid thickness, which is larger for the NEXT thruster.[5]

Table 1 Gridlet geometry and throttling conditions: geometry

Symbol	109-hole gridlet, mm
d_s	1.91
t_s	0.38
ℓ_g	0.66
d_a	1.14
t_a	0.51
ℓ_{cc}	2.21

Table 2 Gridlet geometry and throttling conditions: operating conditions

Symbol	NSTAR	NEXT
Isp	3100 s	4050 s
V_B	1100 V	1830 V
V_a	−180 V	−210 V

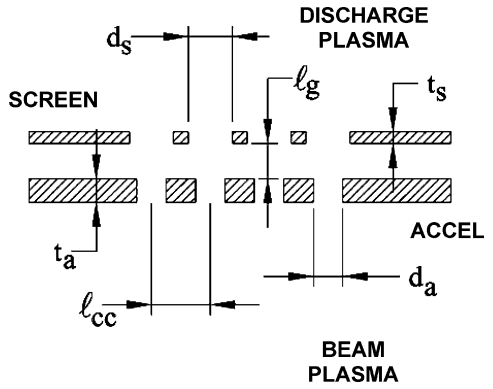

Fig. 2 Gridlet geometry definitions. See Tables 1 and 2 for more information.

The ability of an ion optics system to impart a negative potential throughout the beamlet volume near the axial location of the accelerator grid determines its capacity to stop beam plasma electrons from backstreaming into the discharge chamber. The geometry of a typical ion optics aperture set applies boundary conditions that result in an electrostatic potential saddle point being formed near the axial location of the accelerator grid on the beamlet centerline. The saddle point potential presents the lowest resistance path to electrons on trajectories that could carry them from the beam plasma toward the discharge plasma.[4] The magnitude of the negative voltage that must be applied to the accelerator grid to prevent electron backstreaming, the backstreaming limit, was measured at each beamlet current condition investigated. This measurement was accomplished by 1) setting the accelerator voltage magnitude to a value where no backstreaming occurs, 2) slowly decreasing the accelerator voltage magnitude and simultaneously monitoring the beam current, and 3) analyzing the beam current/accelerator voltage data to determine the voltage where the beam current begins to increase because of backstreaming electron flow.

D. Ion Optics System Evaluation

The vacuum test facility used to evaluate the flat and dished 8-cm-diam C-C ion optics system was 31 cm in diameter and 60 cm long. A Varian 550 turbopump in combination with a roughing pump were used to evacuate the vacuum chamber. Base pressures in the low 10^{-4} Pa (10^{-6} torr) range were readily achievable after running the pumps for 30 min. Under xenon flow rates of 0.6 to 4 sccm, the chamber pressure would rise from 8×10^{-3} to 4×10^{-2} Pa (6×10^{-5} to 3×10^{-4} torr), respectively. Both the flat and dished 8-cm-diam C-C grids were mounted to a laboratory-model 8-cm-diam thruster. The thruster was equipped with a hot filament cathode. All tests were performed by setting the xenon flow rate to a value where the discharge chamber propellant utilization efficiency was $80 \pm 5\%$. Once the thruster was operating at a given beam current and voltage condition, the accelerator voltage magnitude was slowly decreased until electron backstreaming was detected. A typical backstreaming limit measurement data set is plotted in Fig. 3 for illustration purposes. For this study, the onset of backstreaming was defined to occur when the apparent beam current increased by 2.5% above the nominal beam current measured at the start of the test. It is noted that the 2.5% value is arbitrary, and either lower or higher values could have been used. However, it is pointed out that the beam current rose relatively quickly once backstreaming started and different onset definitions from less than 1% up to 10% did not change the measurement results significantly (i.e., ± 10 V). The resolution of the beam current for this study was ± 1 mA. The overall error in the backstreaming limit measurement for the full-scale ion optics systems was ± 10 V as estimated from worst-case error analysis. The dominant error contributing factor was the voltage step size of 5 V that was used to record the data.

In addition to backstreaming measurements made as a function of beam current and voltage, tests were conducted to determine the impingement-limited total voltage over a wide range of beam current

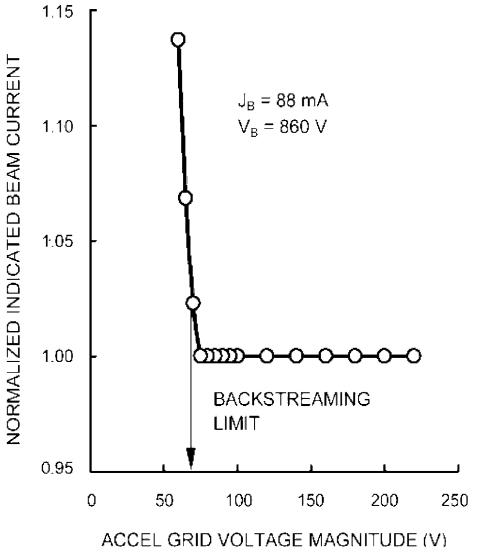

Fig. 3 Typical backstreaming data that were used to determine a backstreaming limit datum for the dished 8-cm-diam grid set.

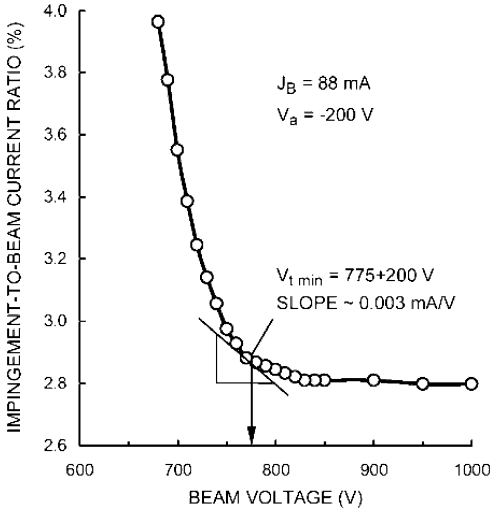

Fig. 4 Typical perveance limit test used to determine an impingement-limited total voltage datum.

values. These perveance limit tests were performed by setting the beam voltage to a value ~300 V above where direct impingement of ions on the accelerator grid would occur and slowly decreasing the beam voltage until the rate of rise of impingement current rose above 0.003 mA/V. This value was chosen to be near the value used by Haag and Soulas[12] and by the resolution of the impingement current and beam voltage measurements. A typical impingement current vs beam voltage plot is shown in Fig. 4. For this beam current operating condition of 88 mA, the impingement current was observed to increase rapidly as the beam voltage was decreased below 775 V [i.e., the magnitude of the impingement current-to-beam voltage slope ($|dJ_a/dV_B|$) increased above 0.003 mA/V]. The overall error in the impingement-limited total voltage was ± 30 V, where the uncertainty was again mostly because of the voltage step size of 10 V that was used to obtain most of the impingement-limited data.

III. Results

Test and analysis results are presented in the following four sections: 1) gridlet test results, 2) performance data collected with both flat and dished 8-cm-diam ion optics systems, 3) propellant throughput calculations, and 4) vibration test results.

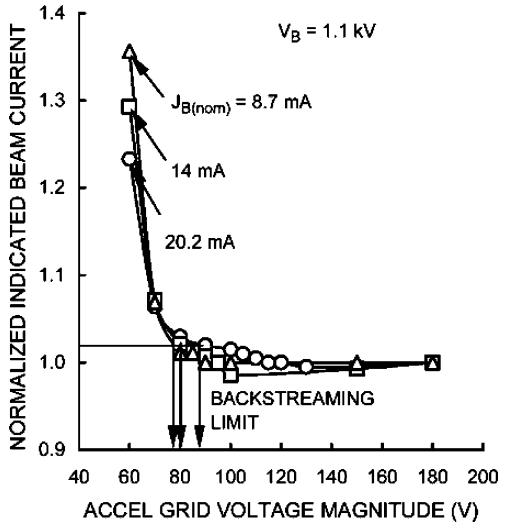

Fig. 5 Typical electron backstreaming data collected with NSTAR carbon-carbon gridlets.

A. Subscale Ion Optics Tests

The 109-aperture C-C gridlets were operated from net accelerating voltages V_B of 1100 V (NSTAR) to 1830 V (NEXT). Three backstreaming curves showing the sudden increase in apparent beam current that occurs at the backstreaming limit are displayed in Fig. 5. The ordinate in this plot is the ratio of beamlet currents measured at $|V_a|$ and at a voltage significantly greater than the backstreaming limit, namely, $|V_a| = 180$ V. At the backstreaming limit, electrons drawn upstream from the beam plasma into the discharge chamber plasma cause the increase in apparent beamlet current. As mentioned earlier, it was decided to define the onset of backstreaming to be when the beam current increased to a value ~2.5% above the beam current measured at $|V_a| = 180$ V. This arbitrary value was chosen to be relatively high to reduce the uncertainty of where backstreaming begins. As indicated in the figure, higher accelerator voltage magnitudes were required to stop electrons from backstreaming through the gridlets when they were operated at higher beam current values.

The backstreaming limit value at $J_{B(\text{nom})} = 20.2$ mA of 88 V is about 50 V lower than backstreaming voltages measured at BOL on the FT2 NSTAR thruster when operated at TH15.[14,15] The average and peak beamlet currents for an NSTAR engine operated at TH15 are ~0.1 and ~0.2 mA, respectively, and the 20.2-mA gridlet operating condition corresponds to 0.19 mA/hole (i.e., 20.2 mA/109 holes). The lower backstreaming voltage result observed in the gridlet test relative to the full thruster test was probably caused by differences in the beam plasma conditions and in how the onset of backstreaming was defined. However, the molybdenum grids used in the NSTAR thruster move considerably closer to one another when they are operated (relative to the spacing when the grids are at room temperature).[16] The gridlet tests described herein were performed at cold spacing gaps, and the low coefficient of thermal expansion of the flat C-C composite material probably caused the gap to remain relatively constant over the temperature range imposed by the gridlet test facility (i.e., ~20 to 225°C). Consequently, the gridlet backstreaming limit data collected at the cold gap spacing are expected to be lower in magnitude than the backstreaming limit measured with dished molybdenum grids. Table 3 contains a list of the backstreaming voltages for the gridlet tests over a range of beamlet currents and net accelerating voltages. Table 3 also lists the backstreaming margins for the NSTAR TH15 operating condition (~90 V) and for the NEXT high-power operating condition (~42 V). The voltage margin is the difference between the accelerator voltage where electron backstreaming occurs and the nominal accelerator voltage.

Figures 6a and 6b show typical crossover and perveance limit data obtained with the 109-hole gridlet set. These data are compared with similar measurements made with a gridlet set fabricated from Poco graphite in Fig. 6a. The Poco graphite gridlet was identical to the C-C gridlet in all respects except it only contained 37 apertures. The similarity between the two gridlet tests is considered to be quite good. An important result of the gridlet tests was the crossover limit behavior at low beamlet currents. A recent 2000-h wear test recently completed at NASA Glenn Research Center on the NEXT thruster indicated that crossover ion erosion was occurring

Table 3 Backstreaming limit and margin data

Operating condition	V_B, V	J_b, mA	V_{BS}, V	V_{margin}, V
NSTAR	1100	0.08	77	103
NSTAR	1100	0.13	81	99
NSTAR	1100	0.19	88	92
NEXT	1830	0.14	168	42
NEXT	1830	0.26	156	54
NEXT	1830	0.34	142	68

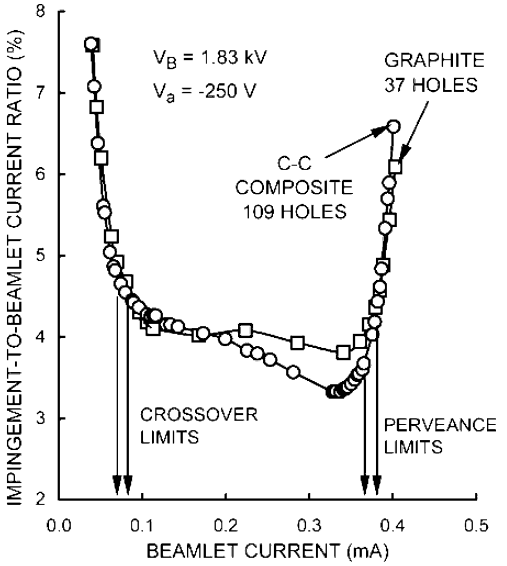

Fig. 6a Typical crossover and perveance impingement limit data collected with NSTAR gridlets fabricated from C-C composites and Poco graphite.

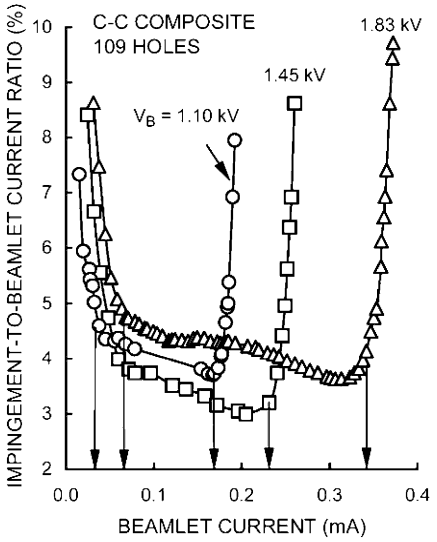

Fig. 6b Crossover and perveance limit data collected with C-C composite gridlets. Grid-to-grid spacing for these data was 10% greater than the nominal NSTAR grid gap at room temperature as confirmed by post-test measurements.

Table 4 Crossover and perveance beamlet current limits

Operating condition	V_B, V	V_a, V	$J_{b,\mathrm{COL}}$, mA	$J_{b,\mathrm{PL}}$, mA
NSTAR	1100	180	0.035	0.18
NEXT	1830	210	0.085	0.36

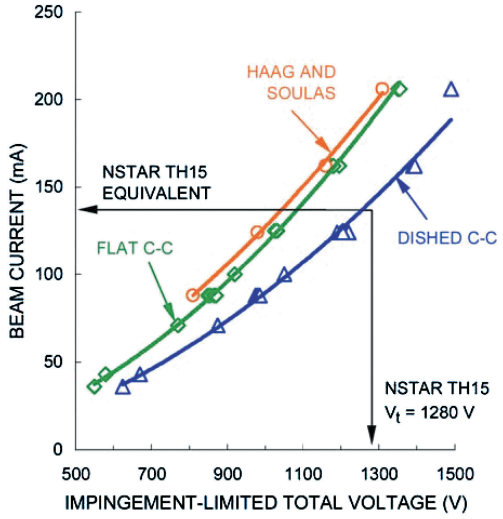

Fig. 7 Comparison of impingement-limited total voltage behavior for flat and dished ion optics systems fabricated from C-C composites and pyrolytic graphite (from Ref. 12).

at ~0.08 mA/hole,[5] which is similar to where the crossover limit was observed in the gridlet tests shown in Fig. 6a. A summary of the crossover and perveance limits is listed in Table 4. As expected, the higher total voltage of the NEXT operating condition results in higher crossover and perveance limits compared to the NSTAR operating condition.

B. Eight-Centimeter-Diameter Ion Optics Performance Measurements

Impingement-limited total voltage measurements are plotted in Fig. 7. The flat C-C grids were observed to perform similarly to the flat pyrolytic grids of Haag and Soulas,[12] which were operated on a masked-down 30-cm-diam NSTAR thruster. The slight difference between the two flat grid systems could be caused by differences in the plasma density variation across the grids. It is expected that the smaller thruster used in this study would have poorer plasma density uniformity across the 8-cm-diam grid compared to the masked-down NSTAR thruster used by Haag and Soulas. This variation would cause the flat and dished C-C grids to be operated at slightly higher beamlet currents on the thruster centerline where the onset of direct impingement of beam ions on the accelerator grid would occur at higher total voltages compared to a thruster with better plasma density uniformity (i.e., a masked-down NSTAR thruster).

The dished C-C grids were observed to operate with less perveance margin compared to the flat C-C and pyrolytic grids. As mentioned earlier, the 8-cm grid set was gapped at a slightly larger distance near the center of the grids because of a localized nonspherical shape, and this larger gap would cause beamlet ions to directly impinge upon the accelerator grid at higher total voltages (compared to the flat grid set).

The backstreaming limit measurements are plotted in Fig. 8 as a function of beam current. The backstreaming voltage was normalized by dividing by the net accelerating voltage (the beam voltage), and a nominal BOL value of this ratio for the NSTAR thruster was 0.14 for the TH15 operating point.[14] The flat C-C grids were observed to backstream at a value close to 0.1 when the beam current per unit area was similar to the NSTAR TH15 operating point. The dished C-C grids were observed to backstream at lower accelerator voltage magnitudes over the entire beam current range where measurements were performed (relative to the flat C-C grids). The larger gap of the dished C-C grids caused them to perform better in terms of preventing backstreaming than the flat C-C grids. The data from Haag and Soulas[12] are shown to be much lower than either of the C-C grids and the NSTAR TH15 BOL value.

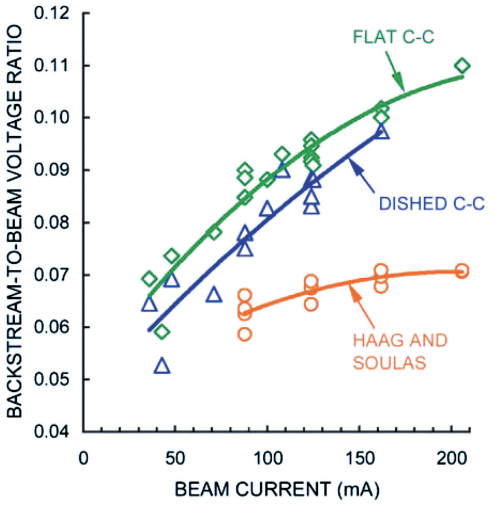

Fig. 8 Comparison of backstreaming voltage limit behavior for flat and dished ion optics systems fabricated from C-C composites and pyrolytic graphite (from Ref. 12).

C. Throughput Enhancement Using Carbon-Based Ion Optics

The sputter yield data measured by Williams et al.[7] and references therein allow one to determine the additional propellant throughput that could be obtained if slower accelerator grid erosion were to occur. The following discussion follows the approach used by Williams et al.

To perform an estimation of the benefits of carbon relative to molybdenum grids, differential sputter yield data could be incorporated into a numerical model of an ion optics system that was able to calculate charge exchange ion generation rates and determine charge-exchange ion trajectories and their subsequent energy and incidence angle as they strike the accelerator grid surface. An effort of this type is beyond the scope of the current study; however, the relative benefit could be estimated to first order by comparing the recession rates of surfaces being subjected to ion bombardment at normal incidence only. The rate of recession of a surface under normal incidence ion bombardment can be expressed as

$$t' = mYj/q\rho \tag{1}$$

The ratio of the recession rate of a molybdenum surface to a carbon surface under identical ion bombardment conditions is

$$\frac{t'_{\mathrm{Mo}}}{t'_C} = \frac{m_{\mathrm{Mo}} Y_{\mathrm{Mo}} \rho_C}{m_C Y_C \rho_{\mathrm{Mo}}} = \beta_{C-\mathrm{Mo}} \tag{2}$$

In Eq. (2) the parameter $\beta_{C-\mathrm{Mo}}$ represents the propellant throughput performance relative to molybdenum assuming that the carbon-based grid could be worn to the same state as the molybdenum grid before failing. To first order, a grid set constructed of carbon that is subjected to normal incidence ion bombardment would have $\beta_{C-\mathrm{Mo}}$ times more propellant throughput capability compared to molybdenum. Plots of β for carbon (or graphite) are shown in Fig. 9. For xenon ion energies between 300 and 1000 eV, grids fabricated from graphite would be expected to last 5 to 6.5 times longer than molybdenum grids. Williams et al.[7] suggest that pyrolytic graphite or C-C grids would be expected to last about 40% longer than grids fabricated from graphite if their bulk density could be made comparable to that of graphite, which has a theoretical maximum

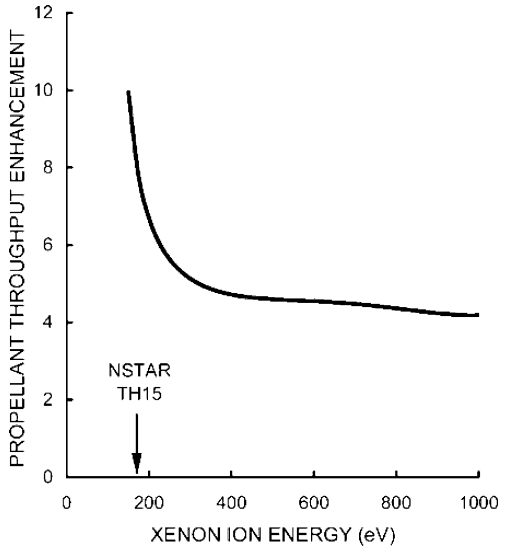

Fig. 9 Propellant throughput factors for carbon-based ion optics systems relative to identical systems fabricated from molybdenum based on sputter erosion rate reductions.

density of 2.3 gm/cm^3.[§§] Significantly greater improvements in relative propellant throughput would be expected for carbon-based ion optics systems if the bombarding ion energy could be held to 250 eV and lower.

D. Random Vibration Test Results

Initially, both the flat and dished 8-cm C-C grids were tested to random vibration levels of 13 g_{rms} and subsequently to 29 g_{rms}. For the dished grid set at a vibration level of about 13 g_{rms}, the first intragrid contact was noted, which was followed by more frequent contacts between vibration test levels from 13 to 29 g_{rms}. Both the dished accelerator and screen electrodes remained structurally intact without any damage or fractures up to the 29 g_{rms} test level. Similarly, the flat electrodes also survived the 13-g_{rms} to 29-g_{rms} tests. The only signs of debris were small amounts of carbon flakes/dust. However, as mentioned earlier, pretest microphotographs revealed the presence of several partial and/or through thickness web fractures in the flat screen grid. These were assumed to have occurred during either handling, machining, or shipping. The fractures were arranged in a chain that followed the grid periphery for about 30 deg of the circumference. Postvibration test inspections detected no new fractures or anomalies, but the visibility of the original fractures did become more apparent.

IV. Conclusions

Results of performance tests were presented on two sets of 8-cm-diam C-C ion optics assemblies designed and fabricated to grid feature geometries that were identical to the NSTAR ion engine. The C-C grids and gridlets were processed using physical vapor deposition to infiltrate and increase the density of the bulk material and coat them with a hard, uniform surface that allowed them to be operated at the high-power throttle points of the NSTAR and NEXT thrusters. Random vibration tests conducted up to 29 g_{rms} indicated that both the flat and dished screen and accelerated grids remained structurally sound. No intragrid contact was noted until the vibration tests were increased above 13 g_{rms}, which was consistent with analytical predictions. Electron backstreaming performance was characterized as a function of beam current and was found to be in good agreement with NSTAR BOL data. Impingement-limited total voltage behavior for the flat grids was observed to be similar to an 8-cm ion optics system fabricated from flat pyrolytic graphite that was reported by Haag and Soulas.[12] The dished grids displayed slightly less total perveance margin because of slightly larger grid-to-grid spacing than nominal NSTAR values near the central regions of the assembly. The test results obtained to date using C-C composites support the feasibility of directly replacing grid assemblies fabricated from molybdenum. Preliminary estimates suggest that propellant throughput of a given ion thruster could be increased by a factor of five by switching from molybdenum to a carbon-based ion optics system, which has lower sputter erosion rates.

[§§]Data available online at http://invsee.asu.edu/nmodules/Carbonmod/density.html. Note that typical high-density graphite (semiconductor grade DFP-1) from Poco graphite has an apparent density of 1.8 gm/cm^3 due to 20% open porosity: http:// www.poco.com/Graphite/dfp.asp.

Acknowledgments

The financial support for this work was provided by Air Force Contract F33615-01-C-5019. Special thanks to Lt. Rodrick Koch, Air Force Research Laboratory/Nonmetallic Materials Division, Wright–Patterson Air Force Base; John Brophy, Jet Propulsion Laboratory, Pasadena, California; Nicole Meckel, Aerojet Redmond Operations, Washington; Kevin Makowski, Lockheed Martin Space Systems Company, Colorado; and Thomas Haag, NASA Glenn Research Center. Discussions with George Soulas, NASA Glenn Research Center, March 2004, on topics related to the NEXT thruster are gratefully acknowledged.

References

[1]Williams, J. D., Laufer, D. M., and Wilbur, P. J., "Experimental Performance Limits on High Specific Impulse Ion Optics," *International Electric Propulsion Conference*, Paper 03-128, March 2003.

[2]Laufer, D. M., Williams, J. D., Farnell, C. C., Shoemaker, P. B., and Wilbur, P. J., "Experimental Evaluation of Sub-Scale CBIO Ion Optics Systems," AIAA Paper 2003-5165, July 2003.

[3]Farnell, C. C., Williams, J. D., and Wilbur, P. J., "Numerical Simulation of Ion Thruster Optics," *International Electric Propulsion Conference*, Paper 03-073, March 2003.

[4]Williams, J. D., Goebel, D. M., and Wilbur, P. J., "A Model of Electron Backstreaming in Ion Thrusters," AIAA Paper 2003-4560, July 2003.

[5]Soulas, G. S., Kamhawi, H., and Patterson, M., "NEXT Ion Engine 2000 h Wear Test Results," AIAA Paper 2004-3791, July 2004.

[6]Goebel, D. M., and Schneider, A. C., "High-Voltage Breakdown and Conditioning of Carbon and Molybdenum Electrodes," *IEEE Transactions on Plasma Science*, Vol. 33, No. 4, 2005, pp. 1136–1148.

[7]Williams, J. D., Johnson, M. L., and Williams, D. D., "Differential Sputtering Behavior of Various Forms of Carbon Under Xenon Bombardment," AIAA Paper 2004-3788, July 2004.

[8]Rawal, S. P., and Koch, R., "Design and Development of Carbon-Carbon Ion-Engine Grids," *Society of Advanced Materials and Processes Exposition, 2003 Technical Conference*, ASM International, Materials Park, OH, Oct. 2003.

[9]Mueller, J., Brophy, J. R., and Brown, D. K., "Design, Fabrication, and Testing of 30-cm Diameter Dished Carbon-Carbon Ion Engine Grids," AIAA Paper 96-3204, July 1996.

[10]Merserole, J. S., and Rorabach, M. E., "Fabrication and Testing of 15-cm C-C Grids with Slit Apertures," AIAA Paper 95-2661, July 1995.

[11]S. Kitamura, S., Hayakawa, Y., Kasai, Y., and Ozaki, T., "Fabrication of Carbon-Carbon Composite Ion Thruster Grids-Improvement of Structural Strength," *International Electric Propulsion Conference*, Paper 97-093, Oct. 1997.

[12]Haag, T. W., and Soulas, G. C., "Performance of 8 cm Pyrolytic-Graphite Ion Thruster Optics," AIAA Paper 2002-4335, July 2002.

[13]Haag, T. W., Patterson, M. J., Rawlin, V., and Soulas, G. C., "Carbon-Based Ion Optics Development at NASA GRC," *International Electric Propulsion Conference*, Paper 2001-094, Oct. 2001.

[14]Sengupta, A., Brophy, J. R., and Goodfellow, K. D., "Status of the Extended Life Test of the Deep Space 1 Flight Spare Ion Engine After 30,352 Hours of Operation," AIAA Paper 2003-4558, July 2003.

[15]Soulas, G., "Improving the Total Impulse Capability of the NSTAR Ion Thruster with Thick-Accelerator-Grid Ion Optics," *International Electric Propulsion Conference*, Paper 01-081, Oct. 2001.

[16]Poeschel, R. L., and Beattie, J. R., "Primary Electric Propulsion Technology Study," NASA CR-159688, Final Rept. on NAS3-21040, Nov. 1979, pp. 135–154.